Flavor symmetry analysis of charmless $B \to VP$ decays

Flavor symmetry analysis of charmless $B \to VP$ decays

Cheng-Wei Chiang[a,b] **and Yu-Feng Zhou**[c,d]

[a]*Department of Physics and Center for Mathematics and Theoretical Physics,*
National Central University, Chungli, Taiwan 320, R.O.C.

[b]*Institute of Physics, Academia Sinica,*
Taipei, Taiwan 115, R.O.C.

[c]*Korea Institute for Advanced Study, Seoul 130-722, Korea*

[d]*Kavli Institute for Theoretical Physics, Institute of Theoretical Physics,*
Chinese Academy of Sciences, Beijing, 100190, P.R. China

E-mail: chengwei@phy.ncu.edu.tw, yfzhou@kias.re.kr

ABSTRACT: Based upon flavor SU(3) symmetry, we perform global fits to charmless B decays into one pseudoscalar meson and one vector meson in the final state. We consider different symmetry breaking schemes and find that the one implied by naïve scaling, where strangeness-conserving and strangeness-changing amplitudes are related by the ratio of appropriate decay constants, is slightly favored over the exact symmetry case. The $(\bar{\rho}, \bar{\eta})$ vertex of the unitarity triangle (UT) constrained by our fits is consistent with other methods within errors. We have found large color-suppressed, electroweak penguin and singlet penguin amplitudes when the spectator quark ends up in the final-state vector meson. Nontrivial relative strong phases are also required to explain the data. The best-fit parameters are used to compute branching ratio and CP asymmetry observables in all of the decay modes, particularly those in the B_s decays to be measured at the Tevatron and LHC experiments.

Contents

1 Introduction

Thanks to the B-factories, a plethora of data on rare hadronic B meson decays have become available in recent years. Because they involve W-mediated charged currents through mixing and/or decay, these decay modes provide particularly useful information on the CP-violating weak phases and magnitudes of elements in the Cabibbo-Kobayashi-Maskawa (CKM) matrix [1, 2] for the quark sector of the standard model (SM). Advances in both experiment and theory have helped us narrow down these parameters to a high precision. Through such efforts, it therefore becomes possible for us to search for evidence of new physics, if any.

Due to the hadronic nature of particles involved in the decays, strong phases associated with the decay amplitudes that are derived from short-distance physics as well as final-state interactions are also important. Even though they cannot be computed from first principles, these phases play a crucial role in direct CP asymmetries. Determination of their pattern and magnitudes in B decays tests our knowledge of strong dynamics in the SM.

An approach utilizing flavor symmetry to relate magnitudes and strong phases of amplitudes [3–7] has been taken to analyze the rare B decay data. It has the advantage of reducing model dependence for computing matrix elements of hadronic transitions, in comparison with the usual perturbative approaches.

In ref. [8], we have updated the analysis for B decays into two charmless pseudoscalar mesons in the final state, and further tested the flavor symmetry assumption by considering several different breaking schemes in the amplitudes. By performing global fits, we find that our results are robust against fluctuations of individual data with large uncertainties, and different schemes have roughly the same predictions.

In this article, we concentrate on the rare $B \to VP$ decays, where V and P denote charmless vector and pseudoscalar mesons, respectively. There have been some numerical works in the perturbation framework of quantum chromodynamics (QCD) to calculate the decay rates and CP asymmetries of these decays over the years. Naïve and general factorization analyses were considered in refs. [9–11]. The QCD factorization (QCDF) method

was employed in refs. [12–17]. The calculations using the perturbative QCD approach are scattered in refs. [18–23]. Recently, the soft-collinear effective theory (SCET) was also used in ref. [24]. In parallel, some attempts that apply the flavor symmetry to the VP decays are given in refs. [24–28].

The $B \to VP$ decay modes present a richer structure than the PP final states because the light spectator quark in B meson can end up in a spin-0 or spin-1 meson, even though the quark-level subprocess is exactly the same. Moreover, the number and precision of observables in these modes (particularly the strangeness-changing ones) have improved considerably in recent years. Totally, there are 52 observables in the VP decays. All the branching ratio and CP asymmetry observables in the strangeness-changing decays of $B^{0,+}$ mesons have been measured. The branching ratio of $\rho^+ K^0$, in particular, provides valuable information on the magnitude of one type of QCD penguin amplitude. In contrast, the observables in the strangeness-conserving transitions are mostly measured in the B^+ decays. Moreover, some data points have shifted by noticeable amounts. For example, the central values of the branching ratios of $B^+ \to \rho^+ \eta^{(\prime)}$, $B^+ \to K^{*+}\eta$, and $K^{*+}\pi^-$ have dropped by about 30% from five years ago. The branching ratios of $B^0 \to \rho^\mp \pi^\pm$ also have moved significantly upward and downward, respectively. Therefore, we consider it timely to re-analyze the data and, at the same time, relax some of the assumptions made in ref. [28] in view of the better data pool, and make predictions for the B_s decay modes which are going to be measured at Tevatron and LHCb.

The structure of this paper is as follows. In section 2, we introduce the notation used in our approach and present both measured observables and amplitude decomposition for the decay modes. In section 3, we show our fitting results of the theory parameters in different schemes. Discussions and predictions based on our fits are given in section 4. Section 5 summarizes our findings in this work.

2 Formalism and notation

For a two-body $B \to VP$ decay process, the magnitude of its invariant decay amplitude M is related to the partial width in the following way:

$$\Gamma(B \to VP) = \frac{|\mathbf{p}|}{8\pi m_B^2}|M|^2 \,, \tag{2.1}$$

where $\mathbf{p}$ is the 3-momentum of the final state particles in the rest frame of the B meson of mass m_B. To relate partial widths to branching ratios, we use the world-average lifetimes $\tau^+ = (1.638 \pm 0.011)$ ps, $\tau^0 = (1.530 \pm 0.009)$ ps, and $\tau_s = (1.437 \pm 0.031)$ ps computed by the Heavy Flavor Averaging Group (HFAG). [1] Each branching ratio quoted in this paper has been CP-averaged.

To perform the flavor amplitude decomposition, we use the following quark content and phase conventions for mesons:

- *Bottom mesons*: $B^0 = d\bar{b}$, $\overline{B}^0 = b\bar{d}$, $B^+ = u\bar{b}$, $B^- = -b\bar{u}$, $B_s = s\bar{b}$, $\overline{B}_s = b\bar{s}$;

---

[1]Updated results and references are tabulated periodically by the Heavy Flavor Averaging Group: http://www.slac.stanford.edu/xorg/hfag/rare.

- *Pseudoscalar mesons*: $\pi^+ = u\bar{d}$, $\pi^0 = (d\bar{d} - u\bar{u})/\sqrt{2}$, $\pi^- = -d\bar{u}$, $K^+ = u\bar{s}$, $K^0 = d\bar{s}$, $\overline{K}^0 = s\bar{d}$, $K^- = -s\bar{u}$, $\eta = (s\bar{s} - u\bar{u} - d\bar{d})/\sqrt{3}$, $\eta' = (u\bar{u} + d\bar{d} + 2s\bar{s})/\sqrt{6}$;

- *Vector mesons*: $\rho^+ = u\bar{d}$, $\rho^0 = (d\bar{d} - u\bar{u})/\sqrt{2}$, $\rho^- = -d\bar{u}$, $\omega = (u\bar{u} + d\bar{d})/\sqrt{2}$, $K^{*+} = u\bar{s}$, $K^{*0} = d\bar{s}$, $\overline{K}^{*0} = s\bar{d}$, $K^{*-} = -s\bar{u}$, $\phi = s\bar{s}$.

The η and η' mesons correspond to octet-singlet mixtures

$$\eta = \eta_8 \cos\theta_0 - \eta_1 \sin\theta_0 , \tag{2.2}$$

$$\eta' = \eta_8 \sin\theta_0 + \eta_1 \cos\theta_0 . \tag{2.3}$$

As shown in ref. [28], varying the mixing angle θ_0 does not improve the quality of fits. For convenience, we fix $\theta_0 = \sin^{-1}(1/3) \simeq 19.5°$ according to the above-mentioned quark contents of η and η'.

We list flavor amplitude decompositions and averaged experimental data for $B \to VP$ decays in tables 2 and 2. Values of measured observables are obtained from the latest 2008 summer results of the HFAG [29] without scale factors.

For the $\rho^\pm \pi^\mp$ modes, the branching ratio reported by the experimental groups is the sum of CP-averaged branching ratio $\mathcal{B}(\rho^\pm \pi^\mp) \equiv \mathcal{B}(\rho^- \pi^+) + \mathcal{B}(\rho^+ \pi^-)$ and the CP asymmetry is defined as $A_{\rho\pi} \equiv (\mathcal{B}(\rho^+ \pi^-) - \mathcal{B}(\rho^- \pi^+))/(\mathcal{B}(\rho^+ \pi^-) + \mathcal{B}(\rho^- \pi^+))$. These quantities can be related to the observables of the individual modes through parameters C and ΔC measured in time-dependent analysis . For example, $\mathcal{B}(\rho^+ \pi^-) = (1 + \Delta C + A_{\rho\pi} C)\mathcal{B}(\rho^\pm \pi^\mp)/2$ and $A_{CP}(\rho^+ \pi^-) = -(A_{\rho\pi} + C + A_{\rho\pi} \Delta C)/(1 + \Delta C + A_{\rho\pi} C)$. A more detailed discussion can be found in ref. [28]. We present the values for individual $\rho^\pm \pi^\mp$ modes in table 2, as calculated from the original HFAG results.

In the present approximation, we consider only five dominant types of independent amplitudes: a "tree" contribution T; a "color-suppressed" contribution C; a "QCD penguin" contribution P; a "flavor-singlet" contribution S, and an "electroweak (EW) penguin" contribution P_{EW}. The first four types are considered as the leading-order amplitudes, while the last one is higher-order in weak interactions. Depending upon which final state meson the spectator quark in the B meson ends up in, we further associate a subscript P or V to the above-mentioned amplitudes. For example, T_P and T_V denote a tree amplitude with the spectator quark of the B meson going into the pseudoscalar and vector meson in the final state, respectively. These two kinds of amplitudes are different in general. In the following, we will suppress the subscripts P, V when discussions apply to both classes of amplitudes of each type.

There are also other types of amplitudes, such as the "color-suppressed EW penguin" diagram P_{EW}^C, "exchange" diagram E, "annihilation" diagram A, and "penguin annihilation" diagram PA. Due to dynamical suppression, these amplitudes are ignored in the analysis.

The QCD penguin amplitude contains three components (apart from the CKM factors): P_t, P_c, and P_u, with the subscript denoting which quark is running in the loop. After imposing the unitarity condition, we can remove the explicit t-quark dependence and are left with two components: $P_{tc} = P_t - P_c$ and $P_{tu} = P_t - P_u$. For simplicity, we assume the t-penguin dominance, so that $P_{tc} = P_{tu} \equiv P$. The same comment applies to the EW penguin and singlet penguin amplitudes, too.

Mode		Flavor Amplitude	BR ($\times 10^{-6}$)	A_{CP}
$B^+ \to$	$\overline{K}^{*0}K^+$	p_P	0.68 ± 0.19	-
	$K^{*+}\overline{K}^0$	p_V	-	-
	$\rho^0\pi^+$	$-\frac{1}{\sqrt{2}}(t_V + c_P + p_V - p_P)$	$8.7^{+1.0}_{-1.1}$	$-0.07^{+0.12}_{-0.13}$
	$\rho^+\pi^0$	$-\frac{1}{\sqrt{2}}(t_P + c_V + p_P - p_V)$	$10.9^{+1.4}_{-1.5}$	0.02 ± 0.11
	$\rho^+\eta$	$-\frac{1}{\sqrt{3}}(t_P + c_V + p_P + p_V + s_V)$	6.9 ± 1.0	0.11 ± 0.11
	$\rho^+\eta'$	$\frac{1}{\sqrt{6}}(t_P + c_V + p_P + p_V + 4s_V)$	$9.1^{+3.7}_{-2.8}$	-0.04 ± 0.28
	$\omega\pi^+$	$\frac{1}{\sqrt{2}}(t_V + c_P + p_P + p_V + 2s_P)$	6.9 ± 0.5	-0.04 ± 0.06
	$\phi\pi^+$	s_P	< 0.24	-
$B^0 \to$	$\overline{K}^{*0}K^0$	p_P	-	-
	$K^{*0}\overline{K}^0$	p_V	< 1.9	-
	$\rho^-\pi^+$	$-(t_V + p_V)$	16.42 ± 1.96^a	0.12 ± 0.06^a
				-0.04 ± 0.13^a
	$\rho^+\pi^-$	$-(t_P + p_P)$	7.58 ± 1.25^a	-0.14 ± 0.12^a
				0.06 ± 0.13^a
	$\rho^0\pi^0$	$-\frac{1}{2}(c_P + c_V - p_P - p_V)$	2.0 ± 0.5	-
	$\rho^0\eta$	$\frac{1}{\sqrt{6}}(c_P - c_V - p_P - p_V - s_V)$	< 1.5	-
	$\rho^0\eta'$	$-\frac{1}{2\sqrt{3}}(c_P - c_V - p_P - p_V - 4s_V)$	< 1.3	-
	$\omega\pi^0$	$\frac{1}{2}(c_P - c_V + p_P + p_V + 2s_P)$	< 0.5	-
	$\omega\eta$	$-\frac{1}{\sqrt{6}}(c_P + c_V + p_P + p_V + 2s_P + s_V)$	< 1.6	-
	$\omega\eta'$	$\frac{1}{2\sqrt{3}}(c_P + c_V + p_P + p_V + 2s_P + 4s_V)$	< 1.9	-
	$\phi\pi^0$	$\frac{1}{\sqrt{2}}s_P$	< 0.28	-
	$\phi\eta$	$-\frac{1}{\sqrt{3}}s_P$	< 0.52	-
	$\phi\eta'$	$\frac{1}{\sqrt{6}}s_P$	< 0.5	-
$B_s \to$	$\overline{K}^{*0}\pi^0$	$-\frac{1}{\sqrt{2}}(c_V - p_V)$	-	-
	$K^{*-}\pi^+$	$-(t_V + p_V)$	-	-
	ρ^+K^-	$-(t_P + p_P)$	-	-
	$\rho^0\overline{K}^0$	$-\frac{1}{\sqrt{2}}(c_P - p_P)$	-	-
	$\overline{K}^{*0}\eta$	$-\frac{1}{\sqrt{3}}(c_V - p_P + p_V + s_V)$	-	-
	$\overline{K}^{*0}\eta'$	$\frac{1}{\sqrt{6}}(c_V + 2p_P + p_V + 4s_V)$	-	-
	$\omega\overline{K}^0$	$\frac{1}{\sqrt{2}}(c_P + p_P + 2s_P)$	-	-
	$\phi\overline{K}^0$	$p_V + s_P$	-	-

^{a} Values obtained using the method outlined in the text and detailed in ref. [28].

Table 1. Flavor amplitude decomposition and measured observables [30–33] of strangeness-conserving $B \to VP$ decays. The time-dependent CP asymmetries $\mathcal{A}$ and $\mathcal{S}$, if applicable, are listed in the first and second rows, respectively.

In physical processes, the above-mentioned flavor amplitudes always appear in specific combinations. To simplify the notation, we therefore define the following unprimed and

primed symbols for $\Delta S = 0$ and $|\Delta S| = 1$ transitions, respectively:

$$
\begin{aligned}
t &\equiv Y_{db}^u T - (Y_{db}^u + Y_{db}^c) P_{EW}^C\,, & t' &\equiv Y_{sb}^u \xi_t T - (Y_{sb}^u + Y_{sb}^c) P_{EW}^C\,, \\
c &\equiv Y_{db}^u C - (Y_{db}^u + Y_{db}^c) P_{EW}\,, & c' &\equiv Y_{sb}^u \xi_c C - (Y_{sb}^u + Y_{sb}^c) P_{EW}\,, \\
p &\equiv -(Y_{db}^u + Y_{db}^c)\left(P - \frac{1}{3} P_{EW}^C\right)\,, & p' &\equiv -(Y_{sb}^u + Y_{sb}^c)\left(\xi_p P - \frac{1}{3} P_{EW}^C\right)\,, \\
s &\equiv -(Y_{db}^u + Y_{db}^c)\left(S - \frac{1}{3} P_{EW}\right)\,, & s' &\equiv -(Y_{sb}^u + Y_{sb}^c)\left(\xi_s S - \frac{1}{3} P_{EW}\right)\,, \quad (2.4)
\end{aligned}
$$

where $Y_{qb}^{q'} \equiv V_{q'q} V_{q'b}^*$ ($q \in \{d, s\}$ and $q' \in \{u, c\}$). Here we also keep the P_{EW}^C amplitude for completeness, though it is ignored in the subsequent analysis. Again, all the above amplitudes are to be associated with subscript P or V, depending on the process. Note that we have explicitly factored out the CKM factors, but leave strong phases inside the amplitudes. This should be distinguished from the notation used in ref. [28], where the CKM factors are absorbed in the amplitudes as well.

From $\Delta S = 0$ to $|\Delta S| = 1$ transitions, we put in SU(3) breaking factors $\xi_{T_{P,V}}, \xi_{C_{P,V}}$, and $\xi_{P_{P,V}}$ for $T_{P,V}$, $C_{P,V}$, and $P_{P,V}$, respectively. If some type of amplitudes is factorizable, the corresponding SU(3) breaking factor is either $f_K/f_\pi = 1.22$ or $f_{K^*}/f_\rho = 1.00$ [34], defined as naïve scaling between strangeness-conserving and strangeness-changing amplitudes. For example, we have for the $B^0 \to K^{*+}\pi^-$ decay:

$$
\mathcal{A}(K^{*+}\pi^-) = -Y_{sb}^u \xi_t T_P + (Y_{sb}^u + Y_{sb}^c)\,\xi_p P_P\,.
$$

This can be obtained from the complete set of flavor amplitude decompositions given in table 2, table 2 and appropriate forms of eqs. (2.4).

In this analysis, the CKM factors are expressed in terms of the Wolfenstein parameterization [35] to $O(\lambda^5)$. Since λ has been determined from kaon decays to high accuracy, we will use the central value 0.2272 quoted by the CKMfitter group [36] as a theory input, and leave A, $\bar{\rho} \equiv \rho(1 - \lambda^2/2)$, and $\bar{\eta} \equiv \eta(1 - \lambda^2/2)$ as fitting parameters to be determined by data.

For the B meson decaying into a CP eigenstate f_{CP}, the time-dependent CP asymmetry is written as

$$
\begin{aligned}
A_{CP}(t) &= \frac{\Gamma(\bar{B}^0 \to f_{CP}) - \Gamma(B^0 \to f_{CP})}{\Gamma(\bar{B}^0 \to f_{CP}) + \Gamma(B^0 \to f_{CP})} \\
&= \mathcal{S}\,\sin(\Delta m_B \cdot t) + \mathcal{A}\,\cos(\Delta m_B \cdot t)\,, \quad (2.5)
\end{aligned}
$$

where Δm_B is the mass difference between the two mass eigenstates of B mesons and t is the decay time measured from the tagged B meson.

3 Fitting analysis

In this section, we present the following two schemes in our fits:

1. exact flavor symmetry for all amplitudes (i.e., $\xi_{T_{P,V}} = \xi_{C_{P,V}} = \xi_{P_{P,V}} = 1$);

2. imposing partial SU(3)-breaking factors on T and C amplitudes only (i.e., $\xi_{T_P,C_P} = f_{K^*}/f_\rho$ and $\xi_{T_V,C_V} = f_K/f_\pi$, while $\xi_{P_P,P_V} = 1$);

Mode	Flavor Amplitude	BR ($\times 10^{-6}$)	A_{CP}
$B^+ \to$ $K^{*0}\pi^+$	p'_P	10.0 ± 0.8	$-0.020^{+0.057}_{-0.061}$
$K^{*+}\pi^0$	$-\frac{1}{\sqrt{2}}(t'_P + c'_V + p'_P)$	6.9 ± 2.3	0.04 ± 0.29
$\rho^0 K^+$	$-\frac{1}{\sqrt{2}}(t'_V + c'_P + p'_V)$	$3.81^{+0.48}_{-0.46}$	$0.417^{+0.081}_{-0.104}$
$\rho^+ K^0$	p'_V	$8.0^{+1.5}_{-1.4}$	-0.12 ± 0.17
$K^{*+}\eta$	$-\frac{1}{\sqrt{3}}(t'_P + c'_V + p'_P - p'_V + s'_V)$	19.3 ± 1.6	0.02 ± 0.06
$K^{*+}\eta'$	$\frac{1}{\sqrt{6}}(t'_P + c'_V + p'_P + 2p'_V + 4s'_V)$	$4.9^{+2.1}_{-1.9}$	$0.30^{+0.33}_{-0.37}$
ωK^+	$\frac{1}{\sqrt{2}}(t'_V + c'_P + p'_V + 2s'_P)$	6.7 ± 0.5	0.02 ± 0.05
ϕK^+	$p'_P + s'_P$	8.30 ± 0.65	0.034 ± 0.044
$B^0 \to$ $K^{*+}\pi^-$	$-(t'_P + p'_P)$	10.3 ± 1.1	-0.25 ± 0.11
$K^{*0}\pi^0$	$\frac{1}{\sqrt{2}}(c'_V - p'_P)$	2.4 ± 0.7	-0.15 ± 0.12
$\rho^+ K^-$	$-(t'_V + p'_V)$	$8.6^{+0.9}_{-1.1}$	0.15 ± 0.06
$\rho^0 K^0$	$-\frac{1}{\sqrt{2}}(c'_P - p'_V)$	$5.4^{+0.9}_{-1.0}$	-0.02 ± 0.29
			0.61 ± 0.26
$K^{*0}\eta$	$-\frac{1}{\sqrt{3}}(c'_V + p'_P - p'_V + s'_V)$	15.9 ± 1.0	0.19 ± 0.05
$K^{*0}\eta'$	$\frac{1}{\sqrt{6}}(c'_V + p'_P + 2p'_V + 4s'_V)$	3.8 ± 1.2	-0.08 ± 0.25
ωK^0	$\frac{1}{\sqrt{2}}(c'_P + p'_V + 2s'_P)$	5.0 ± 0.6	0.32 ± 0.17
			0.45 ± 0.24
ϕK^0	$p'_P + s'_P$	$8.3^{+1.2}_{-1.0}$	0.23 ± 0.15
			$0.44^{+0.17}_{-0.18}$
$B_s \to$ $K^{*+}K^-$	$-(p'_P + t'_P)$	-	-
$K^{*-}K^+$	$-(p'_V + t'_V)$	-	-
$K^{*0}\overline{K}^0$	p'_P	-	-
$\overline{K}^{*0}K^0$	p'_V	-	-
$\rho^0\eta$	$-\frac{1}{\sqrt{6}}c'_P$	-	-
$\rho^0\eta'$	$-\frac{1}{\sqrt{3}}c'_P$	-	-
$\omega\eta$	$-\frac{1}{\sqrt{6}}(c'_P + 2s'_P)$	-	-
$\omega\eta'$	$-\frac{1}{\sqrt{3}}(c'_P + 2s'_P)$	-	-
$\phi\pi^0$	$-\frac{1}{\sqrt{2}}c'_V$	-	-
$\phi\eta$	$\frac{1}{\sqrt{3}}(p'_P + p'_V - c'_V + s'_P - s'_V)$	-	-
$\phi\eta$	$\frac{1}{\sqrt{6}}(2p'_P + 2p'_V + c'_V + 2s'_P + 4s'_V)$	-	-

Table 2. Flavor amplitude decomposition and measured observables [30–33] of strangeness-changing $B \to VP$ decays. The time-dependent CP asymmetries $\mathcal{A}$ and $\mathcal{S}$, if applicable, are listed in the first and second rows, respectively.

We have assumed exact flavor symmetry for the strong phases to reduce independent parameters in our fits. Besides, T_P is fixed to be real and positive in our phase convention (i.e., $\delta_{T_P} = 0$). All the other strong phases are measured with respect to it.

We further divide our fits into two classes: (A) the VP modes that do not involve singlet penguin contributions, and (B) all of the VP modes. As shown in table 2 and

table 2, the modes that contain the singlet penguin amplitudes are those having η, η', ϕ, or ω in the final states.

It is appropriate to list some major differences between the current analysis and ref. [28]. Throughout this analysis, we do not assume any strong phase relation between the EW penguin, singlet penguin, and the QCD penguin amplitudes. Neither do we assume any strong phase relation between the color-suppressed amplitudes and the tree amplitudes. The relative size and phase of P_P and P_V are always kept free. Moreover, we do not assume S_P to be small enough for omission. Instead, we keep it and constrain its magnitude and phase.

In the following, we perform χ^2 fits to the observables in the $B \to VP$ modes as well as $|V_{ub}| = (4.26 \pm 0.36) \times 10^{-3}$ and $|V_{cb}| = (41.63 \pm 0.65) \times 10^{-3}$ [36] for the above-mentioned two schemes. The inclusion of $|V_{ub}|$ and $|V_{cb}|$ helps to fix the values of the Wolfenstein parameters A and $\sqrt{\bar{\rho}^2 + \bar{\eta}^2}$. However, we drop the branching ratio and direct CP asymmetry of the $B^0 \to K^{*0}\pi^0$ decay from the fits because currently the BABAR Collaboration and the Belle Collaboration have a large disagreement in the branching ratio, whose weighted average is $(2.42 \pm 1.16) \times 10^{-6}$ with a scale factor $S = 1.77$. As we will see later, our predictions based on best fits deviate substantially from each of these two observables.

The fit results of theory parameters are summarized in table 3. As given in the table, Scheme 1 of exact SU(3) symmetry is slightly worse than Scheme 2. As defined above, the main difference between these two schemes is in the scaling behavior of T_P and C_P between the strangeness-conserving and strangeness-changing modes. We have also tried other schemes, such as having additional symmetry breaking for amplitude sizes. However, either the fitting quality becomes worse or they involve too large SU(3) breaking (over 30%). We will present our plots and predictions mainly for Scheme 2.

Some general features are observed in these fits. The two types of tree amplitude have roughly the same strong phases, with $|T_V|$ larger than $|T_P|$ by about 50%, largely driven by the branching ratios of $\rho^{\mp}\pi^{\pm}$. The C_V amplitude is 3 to 7 times larger than the C_P amplitude in magnitude. Both of them have sizeable strong phases relative to the tree amplitudes. Moreover, the strong phase of C_P changes abruptly when we enlarge our fitting set from Class (A) to Class (B). They are correlated because they appear in combination in the physical amplitudes.

The best fitted ratios between color-suppressed tree and tree amplitudes are

$$
\begin{array}{ccccc}
 & (A1) & (A2) & (B1) & (B2) \\
|C_V/T_V| = & 0.64 \pm 0.20 & 0.58 \pm 0.18 & 0.81 \pm 0.15 & 0.76 \pm 0.14 \\
|C_P/T_P| = & 0.13 \pm 0.32 & 0.25 \pm 0.31 & 0.22 \pm 0.16 & 0.15 \pm 0.16 \ .
\end{array}
\tag{3.1}
$$

In the four schemes, the central values of the ratio $|C_P/T_P|$ range from 0.13 to 0.25, agreeing with our naïve expectation, even though one still cannot take them seriously due to the large errors coming from the uncertainty in $|C_P|$. On the other hand, the central values for $|C_V/T_V|$ are significantly larger with less uncertainties. The value of $|C_V|$ increases by about 40% from Set (A) to Set (B) though. The four schemes favor $|C_V/T_V|$ in the range of $0.58 \sim 0.76$. As a comparison, the default parameter set of the QCDF approach [16] gives

$$
|C_V/T_V| = 0.158 \pm 0.109 \text{ and } |C_P/T_P| = 0.20 \pm 0.13,
\tag{3.2}
$$

Parameter	Scheme			
	A1	A2	B1	B2
$|T_P|$	0.721 ± 0.088	0.727 ± 0.089	0.785 ± 0.098	0.791 ± 0.100
$|T_V|$	$1.069^{+0.119}_{-0.104}$	$1.070^{+0.119}_{-0.105}$	$1.168^{+0.131}_{-0.116}$	$1.170^{+0.133}_{-0.118}$
δ_{T_V}	1.9 ± 5.7	2.3 ± 5.7	0.4 ± 5.5	0.6 ± 5.4
$|C_P|$	$0.093^{+0.209}_{-0.253}$	0.184 ± 0.223	$0.173^{+0.138}_{-0.108}$	$0.122^{+0.125}_{-0.089}$
δ_{C_P}	-118.9 ± 77.4	-107.7 ± 31.0	133.0 ± 34.2	$149.0^{+72.4}_{-43.0}$
$|C_V|$	$0.688^{+0.226}_{-0.174}$	$0.624^{+0.209}_{-0.154}$	0.945 ± 0.142	0.892 ± 0.139
δ_{C_V}	$-66.0^{+30.3}_{-22.7}$	$-57.0^{+31.3}_{-25.2}$	$-82.0^{+12.0}_{-10.1}$	$-75.9^{+12.6}_{-10.7}$
$|P_P|$	0.084 ± 0.003	0.084 ± 0.003	0.085 ± 0.003	0.085 ± 0.003
δ_{P_P}	-3.9 ± 10.2	-5.7 ± 10.0	-1.0 ± 8.0	-2.6 ± 7.8
$|P_V|$	0.065 ± 0.004	0.063 ± 0.004	0.068 ± 0.004	0.066 ± 0.004
δ_{P_V}	171.7 ± 8.1	172.6 ± 7.7	172.2 ± 7.1	172.5 ± 6.9
$|P_{EW,P}|$	$0.039^{+0.009}_{-0.011}$	$0.039^{+0.009}_{-0.010}$	$0.032^{+0.010}_{-0.013}$	$0.031^{+0.010}_{-0.011}$
$\delta_{P_{EW,P}}$	$56.4^{+10.4}_{-11.6}$	$55.1^{+10.4}_{-11.9}$	$60.9^{+10.0}_{-15.1}$	$59.0^{+10.5}_{-15.8}$
$|P_{EW,V}|$	0.067 ± 0.049	$0.052^{+0.048}_{-0.041}$	$0.096^{+0.027}_{-0.030}$	0.087 ± 0.029
$\delta_{P_{EW,V}}$	$-98.7^{+52.0}_{-23.3}$	$-90.2^{+82.0}_{-26.1}$	$-113.5^{+9.6}_{-8.2}$	$-111.0^{+10.4}_{-8.6}$
$|S_P|$	fixed	fixed	$0.015^{+0.005}_{-0.005}$	$0.014^{+0.004}_{-0.004}$
δ_{S_P}	fixed	fixed	$-133.4^{+16.0}_{-23.9}$	$-139.8^{+16.6}_{-23.5}$
$|S_V|$	fixed	fixed	0.049 ± 0.005	0.048 ± 0.005
δ_{S_V}	fixed	fixed	$-49.4^{+22.2}_{-18.6}$	$-47.7^{+21.5}_{-18.3}$
A	0.807 ± 0.013	0.807 ± 0.013	0.809 ± 0.012	0.809 ± 0.012
$\bar{\rho}$	0.151 ± 0.036	0.146 ± 0.035	0.116 ± 0.030	$0.109^{+0.030}_{-0.028}$
$\bar{\eta}$	0.401 ± 0.030	0.400 ± 0.030	0.373 ± 0.029	0.371 ± 0.030
χ^2/dof	$20.7/8$	$19.9/8$	$44.6/30$	$44.5/30$

Table 3. Fit results (1-σ ranges) of the theory parameters for Classes (A) and (B) in the two schemes defined in the text. The minimal χ^2 value and the number of degrees of freedom (dof) are also given. The amplitudes are given in units of 10^4 eV, and the phases are in degrees.

The large $|C_V/T_V|$ ratio is close to what we have found for $|C/T| \sim 0.65$ in the B decays to two pseudoscalars [8, 37–43]. Even though such values of $|C/T|$ in the PP decays and $|C_V/T_V|$ pose a challenge to perturbative calculations, they seem to follow the simple pattern of factorization in tree and color-suppressed tree amplitudes.

The best fitted ratios between the QCD penguin amplitudes and the tree amplitudes are pretty stable among different schemes considered in this work. The ratios for the four schemes are given by

$$
\begin{array}{ccccc}
& \text{(A1)} & \text{(A2)} & \text{(B1)} & \text{(B2)} \\
|P_V/T_V| = & 0.06 \pm 0.01 & 0.06 \pm 0.01 & 0.06 \pm 0.01 & 0.06 \pm 0.01 \\
|P_P/T_P| = & 0.12 \pm 0.01 & 0.12 \pm 0.01 & 0.11 \pm 0.01 & 0.11 \pm 0.01 \ .
\end{array}
\tag{3.3}
$$

In comparison, the ratio $|P/T| \sim 0.21$ in the PP modes [8]. The strong phase of P_P is the same as T_P within a few degrees, whereas that of P_V is about $180°$ different. This

agrees the expectation of refs. [44–46] and reassures our previous finding [28] using old data. However, it is worth noting that in this work this solution is found even without invoking the $B \to K^*\eta$ decays. The QCDF default values are [16]

$$|P_V/T_V| = 0.035 \pm 0.017 \text{ and } |P_P/T_P| = 0.032 \pm 0.006 \,, \qquad (3.4)$$

and also favors an opposite phase between P_P and P_V amplitudes. Such a phase difference is due to the chiral enhancement that results in a sign flip in the effective coefficients for the QCD penguin amplitudes. Note, however, that the magnitudes of the QCD penguin amplitudes derived in QCDF are significantly smaller than what we find. It has been noticed that they cannot account for some large branching ratios in the QCD penguin-dominated modes [15].

The strong phase between P_P and P_V is about $180°$, with the former roughly in phase with T_P. Such a phase difference produces maximal constructive or destructive interference effects in decay modes that involve both of them. Since the relative phases among the tree- and penguin-type amplitudes are trivial (i.e., $\sim 0°$ or $180°$), as will be seen later, we generally do not expect large direct CP asymmetries in the decay modes involving only them.

For the EW penguin amplitudes, the constraint on $|P_{EW,P}|$ is better than $|P_{EW,V}|$ in Set (A). Nevertheless, the constraint on $|P_{EW,V}|$ improves in Set (B). We note that the strong phases of $P_{EW,P}$ and $P_{EW,V}$ are significantly different from those of P_P and P_V, unlike the assumption made in ref. [28]. It is interesting to notice that $|P_{EW,V}|$ increases by about 50% from fits of Set (A) to fits of Set (B). At the same time, the uncertainty in the strong phase associated with $P_{EW,V}$ improves. In Set (B), $|P_{EW,V}|$ is about 3 times larger than $|P_{EW,P}|$. To one's surprise, $|P_{EW,V}|$ is unexpectedly large, in line with $|C_V|$.

In ref. [28], $P_{EW,P}$ is assumed to have the same strong phase as P_P, whereas the strong phase of $P_{EW,V}$ is assumed to be opposite to that of P_V. In particular, the latter assumption was used because a destructive interference between c'_V and p'_P was required to fit the small branching ratio of the $B^0 \to K^{*0}\pi^0$. Although the current measurement of the branching ratio is not much increased from that time, data on the $B^+ \to K^{*+}\pi^0$, which also involves both c'_V and p'_P amplitudes in a different combination, have now become available. The measured value of $\mathcal{B}(K^{*+}\pi^0)$ is about half the prediction given in ref. [28]. This is an example that the assumption that $P_{EW,V}$ has a strong phase opposite to P_V leads to worse predictions on other observables. We have performed a gloabl fit, including the $B^0 \to K^{*0}\pi^0$ decay data, using the above-mentioned strong phase assumptions as in ref. [28]. Taking Scheme B1 as an example, we find $\chi^2_{\min} = 69.4$ with much worse fitting quality than that given in table 3. The parameters in this fit are (using the same units as in table 3):

$$|T_P| = 0.702^{+0.111}_{-0.094} \,,$$
$$|T_V| = 1.100^{+0.139}_{-0.107} \,, \qquad \delta_{T_V} = -2.5 \pm 5.7 \,,$$
$$|C_P| = 0.422^{+0.203}_{-0.361} \,, \qquad \delta_{C_P} = 104.2^{+11.3}_{-18.7} \,,$$
$$|C_V| = 0.641^{+0.135}_{-0.114} \,, \qquad \delta_{C_V} = -10.0^{+15.5}_{-35.6} \,,$$
$$|P_P| = 0.084 \pm 0.003 \,, \qquad \delta_{P_P} = 4.5^{+8.6}_{-15.9} \,,$$

$$|P_V| = 0.071 \pm 0.004 \,, \qquad\qquad \delta_{P_V} = 170.3^{+7.3}_{-9.8} \,,$$
$$|P_{EW,P}| = 0.011^{+0.004}_{-0.005} \,, \qquad\qquad |P_{EW,V}| = 0.030 \pm 0.008 \,,$$
$$|S_P| = 0.017^{+0.007}_{-0.006} \,, \qquad\qquad \delta_{S_P} = -117.1^{+13.6}_{-33.7} \,,$$
$$|S_V| = 0.029^{+0.008}_{-0.007} \,, \qquad\qquad \delta_{S_V} = 52.0^{+18.9}_{-19.4} \,,$$
$$A = 0.809^{+0.013}_{-0.012} \,, \qquad\qquad \rho = 0.117^{+0.031}_{-0.033} \,, \qquad \eta = 0.378^{+0.027}_{-0.033} \,.$$

As expected, the most affected parameters are the magnitudes and strong phases of C_P, C_V, S_P, and S_V because they appear with $P_{EW,P}$ or $P_{EW,V}$ in physical amplitudes. The magnitudes of $P_{EW,P}$ and $P_{EW,V}$ are also slightly different because of the strong phase choices. Some of the worst observable predictions are

$$A_{CP}(K^{*0}\eta) = 0.04 \,(9.56)\,, \qquad\qquad A_{CP}(\rho^-\pi^+) = -0.04 \,(7.12)\,,$$
$$A_{CP}(K^{*+}\pi^-) = 0.03 \,(6.38)\,, \qquad\qquad A_{CP}(\rho^+\eta) = -0.157 \,(5.88)\,,$$
$$\mathcal{B}(\rho^0\pi^0) = 1.1 \,(3.21)\,, \qquad\qquad \mathcal{B}(\rho^+\eta') = 3.96 \,(2.51)\,,$$

where the numbers in the parentheses are the corresponding $\Delta\chi^2$ contributions. We note in passing that even if we remove the strong phase assumptions of the EW penguin amplitudes while keeping the $B^0 \to K^{*0}\pi^0$ branching ratio and CP asymmetry in the fit, the value of $\chi^2_{\min}$ is still as large as about 58.2, still worse than the fit without the two data points.

As to the singlet penguin amplitudes, we find that S_P is about 3 times smaller than S_V in magnitude. This partly justifies the neglect of the former made in ref. [28], in view of the Okubo-Zweig-Iizuka (OZI) rule. Moreover, if one compares the central values, the S_P amplitude has a strong phase in roughly the opposite direction of P_P and subtends a nontrivial angle from C_P. The S_V amplitude has a $\sim 220°$ phase shift from P_V and deviates from C_V by about $30°$. It is interesting to note that the physical amplitude s_P has a completely constructive interference between S_P and $P_{EW,P}/3$. Also, both types of singlet penguin amplitudes are about half the sizes of the corresponding EW penguin amplitudes.

Here we describe qualitatively how some of the theory parameters are fixed by data, thereby explaining their associated uncertainties. For this, we temporarily concentrate on the modes without involving singlet penguin amplitudes. But the argument can be easily extended to all modes. In our fits, the determination of $|P_P|$ and $|P_V|$ is most precise because they can be directly extracted from the strangeness-changing $B^+ \to K^{*0}\pi^+$ and $\rho^+ K^0$ modes. The next most precise parameters are the magnitudes of tree amplitudes and their phase shifts relative to the QCD penguin amplitudes. They are fixed mainly by the strangeness-conserving $B^0 \to \rho^\pm\pi^\mp$ and to some extent by the strangeness-changing $B^0 \to \rho^+ K^-$ and $K^{*+}\pi^-$ modes. Since no direct CP asymmetry is observed in these modes, the relative strong phases are seen to be trivial.

As the color-suppressed and EW penguin amplitudes of the same type (subscript P or V) always show up in pairs in the physical processes, the determination of their sizes and strong phases becomes trickier. This is because the color-suppressed amplitudes dominate in the $\Delta S = 0$ processes, whereas the EW penguin amplitudes play a greater role in the $|\Delta S| = 1$ decays. This explains why $|C_V|$ is better determined whereas $|P_{EW,V}|$ is not, for $\mathcal{B}(B^+ \to \rho^+\pi^0)$ is more precise than $\mathcal{B}(K^{*+}\pi^0)$. Likewise, the precision on $|C_P|$ is

worse than on $|P_{EW,P}|$ because the combination of $\mathcal{B}(B^+ \to \rho^0 K^+)$ and $\mathcal{B}(B^0 \to \rho^0 K^0)$ is better-determined than $\mathcal{B}(\rho^0 \pi^+)$.

Since the singlet penguin amplitudes are loop-mediated, they are better constrained by the $|\Delta S| = 1$ decay modes. Currently, both charged and neutral ϕK modes have consistent branching ratios and direct CP asymmetries. This basically fixes the magnitude and phase of S_P. In contrast, S_V is constrained in a more involved manner through interference with other amplitudes.

We note in passing that in Class (A), we have also found other sets of parameters that render smaller $\chi^2_{\min}$ in the fits. They are not listed in the tables because they are not favored once the modes involving the singlet penguin amplitudes are taken into account. A distinctive feature of such solutions from the above-mentioned ones is that either the relative strong phase between P_P and P_V is close to zero or that between T_P and T_V is close to $180°$. In the former case, an interesting feature is that the ratios $|C_P/T_P| = 0.57 \pm 0.43$ and $|C_V/T_V| = 0.49 \pm 0.12$ in Scheme 2. They become comparable to each other, but still much larger than the usual perturbative expectation. In the latter case, we obtain a somewhat small $\rho = 0.08$.

In figure 1, we show the contours of the $(\bar{\rho}, \bar{\eta})$ vertex at the 1-σ and 95% confidence level (CL) obtained in our fits. The plots in the upper row are obtained from fits to modes without involving the singlet penguin amplitudes. In this case, our favored region of the vertex is slightly higher than that given by the CKMfitter [36] and UTfit [47]. The plots in the lower row are obtained from global fits to all the VP modes. Comparing to the upper row, we see that the favored region in the global fit shifts lower and to the left on the $\bar{\rho}$-$\bar{\eta}$ plane. In this case, the preferred value of β agrees with other methods, while the value of γ is slightly larger. The best fitted three angles in the UT are

$$
\begin{aligned}
\alpha &= (83 \pm 8)° \quad \text{or} \quad 72° < \alpha < 99° (95\%\text{CL}) \,, \\
\beta &= (26 \pm 2)° \quad \text{or} \quad 18° < \beta < 30° (95\%\text{CL}) \,, \\
\gamma &= (71 \pm 5)° \quad \text{or} \quad 62° < \gamma < 78° (95\%\text{CL})
\end{aligned}
\tag{3.5}
$$

for Scheme (A2), and

$$
\begin{aligned}
\alpha &= (84 \pm 6)° \quad \text{or} \quad 77° < \alpha < 95° (95\%\text{CL}) \,, \\
\beta &= (23 \pm 2)° \quad \text{or} \quad 18° < \beta < 23° (95\%\text{CL}) \,, \\
\gamma &= (73 \pm 4)° \quad \text{or} \quad 67° < \gamma < 81° (95\%\text{CL})
\end{aligned}
\tag{3.6}
$$

for Scheme (B2).

The best-fitted UT vertex from the VP modes is highly consistent with the one from the PP modes. When the fits do not involve singlet penguin amplitudes, both VP and PP data favor a slightly larger $\gamma \simeq 70°$ and a larger $\beta \simeq 26°$. After including the modes involving the singlet penguin amplitudes, the best fitted γ becomes even larger while β reduces to the value consistent with the $B \to (c\bar{c})K_S$ measurements.
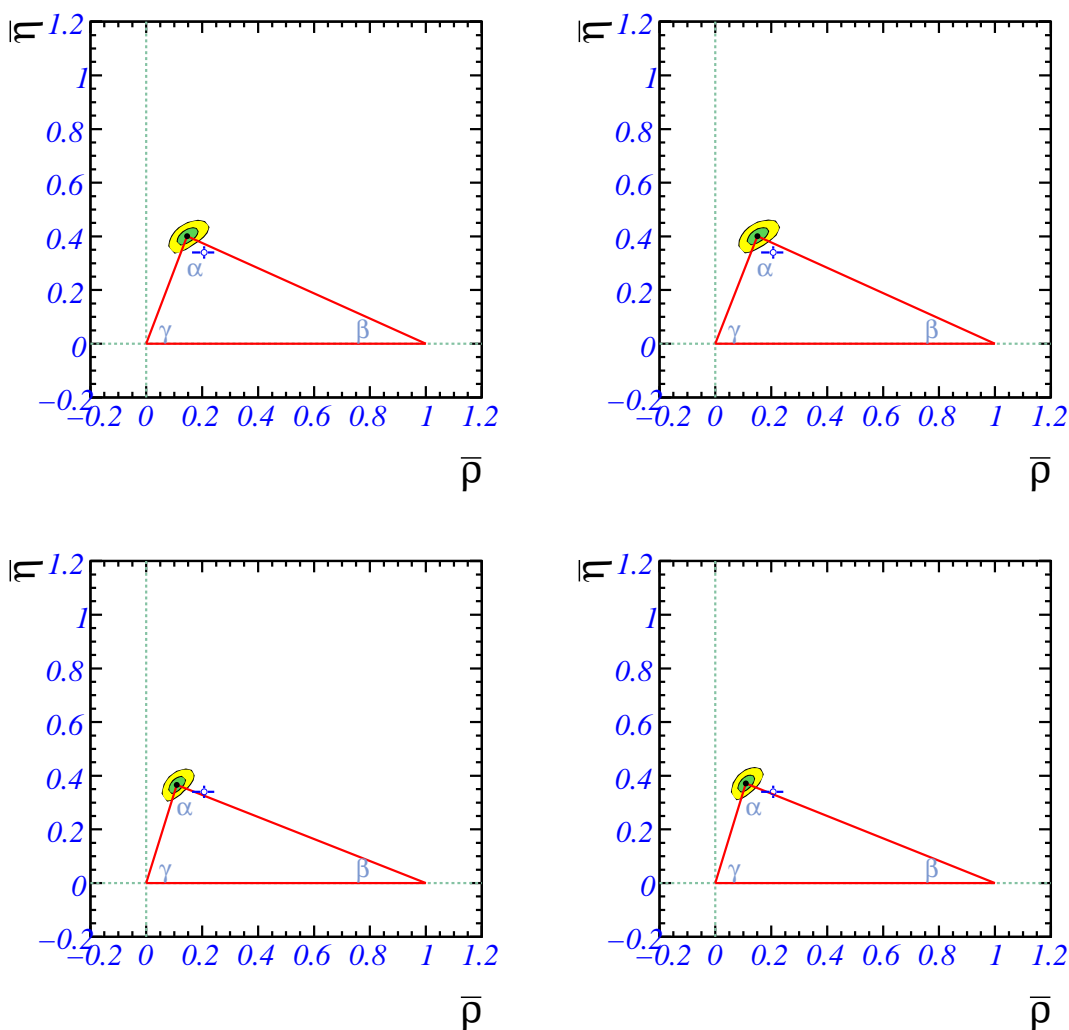
Figure 1. The 1-σ and 95% CL contours of the $(\bar{\rho}, \bar{\eta})$ vertex obtained from fits using the observed VP modes that do not involve the singlet penguin amplitudes (upper row) and using all of the observed VP modes (lower row). The plots in the left (right) column assume Scheme 1 (Scheme 2) defined in the text. The 1-σ range given by the CKMfitter is indicated by the cross in each plot.

4 Discussions

There are two sets of decay modes that can provide a good test for the SU(3) symmetry. One set contains the $B^+ \to K^{*0}\pi^+$, $B^+ \to \overline{K}^{*0}K^+$, $B^0 \to \overline{K}^{*0}K^0$, and $B_s \to K^{*0}\overline{K}^0$ modes. The other set contains the $B^+ \to \rho^+ K^0$, $B^+ \to K^{*+}\overline{K}^0$, $B^0 \to K^{*0}\overline{K}^0$, and $B_s \to \overline{K}^{*0}K^0$ modes. They all involve only the P_P or P_V amplitude, where we have neglected the $P_{EW,P}^C$ or $P_{EW,V}^C$ amplitude in the analysis as said before. However, this argument still applies if the color-suppressed EW penguin amplitude is included because it scales in the same way as the QCD penguin amplitude. Currently, only the $B^+ \to K^{*0}\pi^+$ and $B^+ \to \rho^+ K^0$ modes are observed, and their branching ratios are measured at $\mathcal{O}(10^{-5})$

	Mode	BR ($\times 10^{-6}$)	A_{CP}	$\mathcal{S}$
$B_{u,d} \rightarrow$	$\rho^- \pi^+$	$16.59 \pm 4.01 \; (-0.09)$	$-0.042 \pm 0.041 \; (2.698)$	$0.010 \pm 0.173 \; (-0.384)$
	$\rho^+ \pi^-$	$7.52 \pm 1.97 \; (0.05)$	$0.049 \pm 0.086 \; (-1.576)$	$0.082 \pm 0.166 \; (-0.171)$
	$\rho^0 \pi^0$	$1.97 \pm 0.94 \; (0.06)$	$0.035 \pm 0.179 \; (-)$	$-0.064 \pm 0.297 \; (-)$
	$\rho^+ \pi^0$	$10.94 \pm 3.87 \; (-0.03)$	$-0.011 \pm 0.193 \; (0.277)$	$-$
	$\rho^0 \pi^+$	$8.81 \pm 2.61 \; (-0.11)$	$-0.121 \pm 0.090 \; (0.407)$	$-$
	$\bar{K}^{*0} K^0$	$0.47 \pm 0.05 \; (-)$	$0 \; (-)$	$-$
	$K^{*0} \bar{K}^0$	$0.27 \pm 0.04 \; (-)$	$0 \; (-)$	$-$
	$\bar{K}^{*0} K^+$	$0.50 \pm 0.05 \; (0.94)$	$0 \; (-)$	$-$
	$K^{*+} \bar{K}^0$	$0.29 \pm 0.04 \; (-)$	$0 \; (-)$	$-$
	$\rho^+ K^-$	$8.89 \pm 1.13 \; (-0.29)$	$0.094 \pm 0.094 \; (0.926)$	$-$
	$\rho^0 K^0$	$5.65 \pm 1.21 \; (-0.26)$	$0.076 \pm 0.031 \; (-0.331)$	$0.824 \pm 0.047 \; (-0.822)$
	$\rho^+ K^0$	$6.08 \pm 0.79 \; (1.33)$	$0 \; (-0.706)$	$-$
	$\rho^0 K^+$	$3.80 \pm 0.96 \; (0.03)$	$0.382 \pm 0.119 \; (0.401)$	$-$
	$K^{*0} \pi^0$	$6.59 \pm 3.85 \; (-5.99)$	$-0.330 \pm 0.120 \; (1.500)$	$-$
	$K^{*+} \pi^-$	$8.87 \pm 0.76 \; (1.30)$	$-0.043 \pm 0.075 \; (-1.882)$	$-$
	$K^{*0} \pi^+$	$10.64 \pm 0.82 \; (-0.80)$	$0 \; (-0.339)$	$-$
	$K^{*+} \pi^0$	$7.00 \pm 4.49 \; (-0.04)$	$-0.081 \pm 0.272 \; (0.418)$	$-$
$B_s \rightarrow$	$\rho^+ K^-$	$6.89 \pm 1.81 \; (-)$	$0.049 \pm 0.086 \; (-)$	$-$
	$\rho^0 \bar{K}^0$	$0.39 \pm 0.07 \; (-)$	$0.929 \pm 0.195 \; (-)$	$-0.357 \pm 0.528 \; (-)$
	$K^{*-} \pi^+$	$15.22 \pm 3.68 \; (-)$	$-0.042 \pm 0.041 \; (-)$	$-$
	$\bar{K}^{*0} \pi^0$	$2.60 \pm 1.25 \; (-)$	$-0.134 \pm 0.328 \; (-)$	$-$
	$K^{*-} K^+$	$7.45 \pm 0.93 \; (-)$	$0.085 \pm 0.084 \; (-)$	$-$
	$K^{*+} K^-$	$8.16 \pm 0.70 \; (-)$	$-0.041 \pm 0.072 \; (-)$	$-$
	$\bar{K}^{*0} K^0$	$5.21 \pm 0.68 \; (-)$	$0 \; (-)$	$-$
	$K^{*0} \bar{K}^0$	$9.11 \pm 0.70 \; (-)$	$0 \; (-)$	$-$

Table 4. Predicted $B_{u,d,s}$ decay observables in Scheme (A2). Numbers in the parentheses are the pulls of theory predictions from the current experimental data.

level. It is thus very helpful to measure any of the K^*K modes in this respect. Using the fit results in Scheme (A2) and in units of 10^{-6}, we predict the branching ratios for the first set to be 10.64 ± 0.82, 0.50 ± 0.05, 0.47 ± 0.05, and 9.11 ± 0.70, respectively. The branching ratios for the second set are 6.08 ± 0.79, 0.29 ± 0.04, 0.27 ± 0.04, and 5.21 ± 0.68 in units of 10^{-6}, respectively. These $B_{u,d} \rightarrow K^*K$ modes are somewhat difficult to measure due to the Cabibbo suppression. However, the $B_s \rightarrow K^*K$ modes should be within the reach of the LHCb and Tevatron Run-II experiments.

Although the $B^+ \rightarrow \phi \pi^+$ and $B^0 \rightarrow \phi \pi^0, \phi \eta, \phi \eta'$ modes directly constrain the size of s_P, their branching ratios are expected to be about $\mathcal{O}(10^{-8})$ or smaller. Therefore, they are beyond the current probes.

In the following, we would like to point out some persistent problems encountered in our fits to the current data. In ref. [28], the rate difference relations [48]:

$$\Gamma(B^0 \rightarrow \rho^- \pi^+) - \Gamma(\bar{B}^0 \rightarrow \rho^+ \pi^-) = \frac{f_\pi}{f_K} \left[\Gamma(\bar{B}^0 \rightarrow \rho^+ K^-) - \Gamma(B^0 \rightarrow \rho^+ K^-) \right], \quad (4.1)$$

$$\Gamma(B^0 \rightarrow \rho^+ \pi^-) - \Gamma(\bar{B}^0 \rightarrow \rho^- \pi^+) = \frac{f_\rho}{f_{K^*}} \left[\Gamma(\bar{B}^0 \rightarrow K^{*-} \pi^+) - \Gamma(B^0 \rightarrow K^{*+} \pi^-) \right] \quad (4.2)$$

have been found to be barely and loosely obeyed, respectively, by the data at that time. Using the current data and in terms of the branching ratios, eqs. (4.1) and (4.2) give in units of 10^{-6}, respectively,

$$-3.9 \pm 2.0 \stackrel{?}{=} 2.1 \pm 0.9 , \tag{4.3}$$

$$2.1 \pm 1.9 \stackrel{?}{=} -4.9 \pm 2.2 . \tag{4.4}$$

The first one is still not obeyed at about 2.7σ level. This difference comes from the CP asymmetries of $B^0 \to \rho^-\pi^+$ and $\rho^+ K^-$, both at about 2σ level. To further check the equality in the second equation relies on more precise determinations in the CP asymmetries of $B^0 \to K^{*+}\pi^-$ and $B^0 \to K^{*+}\pi^-$.

Another problem is $\mathcal{B}(B^+ \to \rho^+\eta')/\mathcal{B}(B^+ \to \rho^+\eta) \simeq 1.3 \pm 0.5$, which is very different from our expectation of about $1/2$ based upon the mixing angle we assume for η and η' and assuming that s_V is negligible for $\Delta S = 0$ decays. The problem comes from the large branching ratio of $B^+ \to \rho^+\eta'$, as indicated by the pull in table 5. A similar relation can be found for $\mathcal{B}(B^0 \to \rho^0\eta)/\mathcal{B}(B^0 \to \rho^0\eta')$, $\mathcal{B}(B^0 \to \omega^0\eta)/\mathcal{B}(B^0 \to \omega^0\eta')$, $\mathcal{B}(B_s \to \rho^0\eta)/\mathcal{B}(B_s \to \rho^0\eta')$, and $\mathcal{B}(B_s \to \omega\eta)/\mathcal{B}(B_s \to \omega\eta')$ too. However, these modes may be difficult to measure.

A new problem would occur between the $B^+ \to \rho^0 K^+$ and ωK^+ modes that differ by $\sqrt{2}s'_P$ if s'_P is vanishingly small. In that case, the ratio of their branching ratios should be close to 1 [45]. However, the current data imply 0.57 ± 0.08. With the fitted $S_P \simeq 140\,\mathrm{eV}$, the predicted ratio is $\simeq 0.61$. Consequently, a non-vanishing S_P is preferred.

Another puzzle comes from the CP asymmetry of $B^0 \to K^{*0}\eta$ because it is measured to be non-zero at an almost 4σ level. This is quite different from a closely related mode, $B^+ \to K^{*+}\eta$, whose CP asymmetry is consistent with zero. Their values should not be so different because they only differ by a small tree amplitude.

We make predictions for the observables of all the B^+, B^0 and B_s decays using the extracted parameters given in table 3. In table 4, we only include modes without involving the singlet penguin amplitudes as they are based on Scheme (A2). Table 5 and table 6 cover all the decay modes as they are based on Scheme (B2). The column of A_{CP} refers to either the direct CP asymmetry or $\mathcal{A}$ in eq. (2.5) of the corresponding mode. The numbers in the parentheses are calculated pulls of the theory predictions from experimental observations. They indicate the $\Delta\chi^2$ contributions of individual quantities.

Several observables in table 5 have pulls larger than, say 1.5. Most of them are in the CP asymmetries. It is less clear about their importance as current precision on these data points is not satisfactory. We are then left with two branching ratio predictions with large pulls. The problem with $\rho^+\eta'$ has been mentioned above. As commented before, we do not include the branching ratio and CP asymmetry of the $B^0 \to K^{*0}\pi^0$ in the fits of this work. Its predicted branching ratios in tables 4 and 5 based on the best fits are quite different from the current quotes of averages in table 2, and need further experimental confirmation.

In table 5, our predictions of $\mathcal{B}(B^0 \to \rho^0\eta) = 1.87 \pm 0.64$ and $\mathcal{B}(B^0 \to \omega\pi^0) = 2.82 \pm 0.99$ are larger than the current upper bounds of 1.5 and 0.5, respectively, in units of 10^{-6}. The branching ratio predictions of the other yet-measured modes are all consistent with current 95% upper bounds.

For the B_s decays, we predict large direct CP asymmetries $A_{CP}(\overline{K}^{*0}\eta) \simeq 0.73$ and $A_{CP}(\overline{K}^{*0}\eta') \simeq -0.79$, a result of interference between the large color-suppressed amplitude C_V and the QCD penguin amplitudes. We also predict large branching ratios, in unit of 10^{-6}, $\mathcal{B}(\phi\eta') \simeq 8.47$, $\mathcal{B}(K^{*-}\pi^+) \simeq 15.21$, $\mathcal{B}(K^{*\pm}K^\mp) \simeq 8$, and $\mathcal{B}(K^{*0}\overline{K}^0) \simeq 9.54$. In these modes, the branching ratios can reach $\mathcal{O}(10^{-5})$ or more, as they involve either T_V for $\Delta S = 0$ or P_P for $|\Delta S| = 1$ transitions.

As given in table 3 and mentioned before, the central values of the sizes and strong phases associated with C_P, C_V and $P_{EW,V}$ change noticeably between Set (A) and Set (B). More explicitly, C_P reduces by about 34% in size and changes significantly in strong phase. Both C_V and $P_{EW,V}$ increase by about 43% and 67% in size, respectively, and differ little in strong phase. Therefore, one can see that predictions of modes involving mainly these amplitudes differ substantially between table 4 and tables 5, 6, as far as the central values are concerned. For example, the direct CP asymmetry of $B^0 \to \rho^0 K^0$ (involving $c'_P - p'_V$) changes sign mainly because of the change in the strong phase of C_P. This effect becomes more significant in observables associated with $B_s \to \rho^0 \bar{K}^0$ (involving $c_P - p_P$) as C_P is the dominant component. The facts that the predicted $\mathcal{B}(B^0 \to K^{*0}\pi^0)$ is roughly doubled and that $\mathcal{B}(B_s \to \bar{K}^{*0}\pi^0)$ becomes larger by 64% are due to the increases in $|C_V|$ and $|P_{EW,V}|$.

5 Summary

We have updated the global analysis of charmless $B \to VP$ decays in the framework of flavor SU(3) symmetry using the latest experimental data. Moreover, we consider different SU(3) breaking schemes for the sizes of flavor amplitudes based upon naïve scaling assumption. Our result shows that the symmetry-breaking scheme (Scheme 2 defined in the text) is favored by the χ^2 fits, but its difference from the exact symmetry scheme (Scheme 1) is small. The UT vertex $(\bar{\rho}, \bar{\eta})$ extracted using these modes is consistent with our previous analysis using the PP modes [8], and also agrees with other methods within errors [36, 47]. However, we note that a slightly larger weak phase γ is favored by our global analysis.

In the fits to modes without involving the singlet penguin amplitudes, we note that there are two sets of solutions with minimal χ^2 values. In one set, the P_P and P_V amplitudes have almost the same strong phases. In the other set, they have almost opposite strong phases. The latter is favored when one also includes modes involving the singlet penguin amplitudes. Moreover, we find in the latter case that the ratio C_V/T_V is about 0.6 - 0.7, similar to the C/T ratio in the PP modes. Correspondingly, the $P_{EW,V}$ and S_V amplitudes are unexpectedly large. These facts are seen to be a challenge to perturbative approaches.

We point out that a set of decay modes that involve only the QCD penguin amplitude can be used to test our flavor SU(3) assumption. Among those modes, the $B_s \to K^{*0}\overline{K}^0$ and $\overline{K}^{*0}K^0$ modes should be within the reach of the LHCb and Tevatron Run-II experiments.

We also mention the persistent problems that the CP rate differences in $B^0 \to \rho^-\pi^+$ and in $B^0 \to \rho^+K^-$ do not follow our expectation from factorization and that the observed branching ratio of $B^+ \to \rho^+\eta'$ is too large to be accommodated in our approach. Further investigations of $\mathcal{B}(B^0 \to K^{*0}\pi^0)$ and $A_{CP}(B^0 \to K^{*0}\eta)$ are required.

Mode	BR ($\times 10^{-6}$)	A_{CP}	$\mathcal{S}$
$\rho^-\pi^+$	$16.57 \pm 4.18 \; (-0.08)$	$-0.038 \pm 0.041 \; (2.630)$	$0.070 \pm 0.166 \; (-0.843)$
$\rho^+\pi^-$	$7.32 \pm 1.98 \; (0.21)$	$0.024 \pm 0.072 \; (-1.363)$	$0.084 \pm 0.160 \; (-0.187)$
$\rho^0\pi^0$	$1.91 \pm 0.79 \; (0.19)$	$0.259 \pm 0.148 \; (-)$	$0.115 \pm 0.249 \; (-)$
$\rho^+\pi^0$	$11.12 \pm 2.99 \; (-0.15)$	$-0.026 \pm 0.128 \; (0.415)$	$-$
$\rho^0\pi^+$	$8.27 \pm 2.42 \; (0.41)$	$-0.192 \pm 0.099 \; (0.977)$	$-$
$\rho^0\eta$	$1.87 \pm 0.64 \; (-)$	$0.109 \pm 0.153 \; (-)$	$-0.336 \pm 0.199 \; (-)$
$\rho^0\eta'$	$0.52 \pm 0.15 \; (-)$	$-0.396 \pm 0.291 \; (-)$	$-0.587 \pm 0.222 \; (-)$
$\rho^+\eta$	$7.16 \pm 2.03 \; (-0.26)$	$0.165 \pm 0.103 \; (-0.502)$	$-$
$\rho^+\eta'$	$3.79 \pm 0.98 \; (1.63)$	$-0.071 \pm 0.240 \; (0.110)$	$-$
$\omega\pi^0$	$2.82 \pm 0.99 \; (-)$	$0.293 \pm 0.132 \; (-)$	$-0.094 \pm 0.216 \; (-)$
$\omega\pi^+$	$7.02 \pm 2.23 \; (-0.25)$	$0.020 \pm 0.075 \; (-0.993)$	$-$
$\omega\eta$	$1.27 \pm 0.51 \; (-)$	$-0.016 \pm 0.179 \; (-)$	$-0.360 \pm 0.227 \; (-)$
$\omega\eta'$	$0.76 \pm 0.25 \; (-)$	$-0.624 \pm 0.285 \; (-)$	$-0.511 \pm 0.302 \; (-)$
$\phi\pi^0$	$0.02 \pm 0.01 \; (-)$	$0 \; (-)$	$0 \; (-)$
$\phi\pi^+$	$0.04 \pm 0.02 \; (-)$	$0 \; (-)$	$-$
$\phi\eta$	$0.01 \pm 0.01 \; (-)$	$0 \; (-)$	$0 \; (-)$
$\phi\eta'$	$0.01 \pm 0.00 \; (-)$	$0 \; (-)$	$0 \; (-)$
$\bar{K}^{*0}K^0$	$0.52 \pm 0.05 \; (-)$	$0 \; (-)$	$-$
$K^{*0}\bar{K}^0$	$0.31 \pm 0.04 \; (-)$	$0 \; (-)$	$-$
$\bar{K}^{*0}K^+$	$0.55 \pm 0.05 \; (0.67)$	$0 \; (-)$	$-$
$K^{*+}\bar{K}^0$	$0.33 \pm 0.04 \; (-)$	$0 \; (-)$	$-$
ρ^+K^-	$9.21 \pm 1.04 \; (-0.61)$	$0.082 \pm 0.089 \; (1.128)$	$-$
ρ^0K^0	$5.06 \pm 1.10 \; (0.36)$	$-0.041 \pm 0.045 \; (0.072)$	$0.766 \pm 0.052 \; (-0.598)$
ρ^+K^0	$6.70 \pm 0.74 \; (0.90)$	$0 \; (-0.706)$	$-$
ρ^0K^+	$4.02 \pm 0.82 \; (-0.44)$	$0.382 \pm 0.126 \; (0.398)$	$-$
$\omega\bar{K}^0$	$4.62 \pm 1.01 \; (0.63)$	$0.033 \pm 0.048 \; (1.690)$	$0.700 \pm 0.054 \; (-1.040)$
ωK^+	$6.64 \pm 1.27 \; (0.13)$	$0.029 \pm 0.092 \; (-0.190)$	$-$
ϕK^0	$7.43 \pm 1.21 \; (0.79)$	$0 \; (1.533)$	$0.737 \pm 0.043 \; (-1.699)$
ϕK^+	$7.96 \pm 1.30 \; (0.53)$	$0 \; (0.773)$	$-$
$K^{*0}\pi^0$	$13.85 \pm 4.76 \; (-16.36)$	$-0.294 \pm 0.078 \; (1.201)$	$-$
$K^{*+}\pi^-$	$9.57 \pm 0.72 \; (0.66)$	$-0.019 \pm 0.057 \; (-2.104)$	$-$
$K^{*0}\pi^+$	$11.14 \pm 0.77 \; (-1.43)$	$0 \; (-0.339)$	$-$
$K^{*+}\pi^0$	$7.09 \pm 3.11 \; (-0.08)$	$-0.151 \pm 0.164 \; (0.660)$	$-$
$K^{*0}\eta$	$16.72 \pm 2.44 \; (-0.82)$	$0.162 \pm 0.049 \; (0.560)$	$-$
$K^{*0}\eta'$	$4.16 \pm 1.56 \; (-0.30)$	$0.159 \pm 0.150 \; (-0.954)$	$-$
$K^{*+}\eta$	$17.30 \pm 2.58 \; (1.25)$	$0.070 \pm 0.064 \; (-0.837)$	$-$
$K^{*+}\eta'$	$4.34 \pm 1.64 \; (0.28)$	$-0.027 \pm 0.228 \; (0.933)$	$-$

Table 5. Predicted $B_{u,d}$ decay observables in Scheme (B2). Numbers in the parentheses are the pulls of theory predictions from the current experimental data.

Mode	BR ($\times 10^{-6}$)	A_{CP}	$\mathcal{S}$
$\rho^0 \eta$	0.21 ± 0.14 $(-)$	-0.156 ± 0.123 $(-)$	-0.731 ± 0.092 $(-)$
$\rho^0 \eta'$	0.42 ± 0.26 $(-)$	-0.156 ± 0.123 $(-)$	-0.731 ± 0.092 $(-)$
$\rho^+ K^-$	6.71 ± 1.81 $(-)$	0.024 ± 0.072 $(-)$	$-$
$\rho^0 \bar{K}^0$	0.24 ± 0.10 $(-)$	-0.128 ± 0.773 $(-)$	0.926 ± 0.283 $(-)$
$\omega \eta$	0.07 ± 0.06 $(-)$	0.243 ± 0.234 $(-)$	-0.624 ± 0.195 $(-)$
$\omega \eta'$	0.13 ± 0.12 $(-)$	0.243 ± 0.234 $(-)$	-0.624 ± 0.195 $(-)$
$\omega \bar{K}^0$	0.27 ± 0.14 $(-)$	0.302 ± 0.629 $(-)$	-0.856 ± 0.331 $(-)$
$\phi \pi^0$	2.80 ± 1.80 $(-)$	-0.250 ± 0.121 $(-)$	-0.451 ± 0.131 $(-)$
$\phi \eta$	2.35 ± 1.53 $(-)$	-0.073 ± 0.142 $(-)$	-0.341 ± 0.174 $(-)$
$\phi \eta'$	8.47 ± 2.55 $(-)$	0.096 ± 0.061 $(-)$	-0.626 ± 0.054 $(-)$
$\phi \bar{K}^0$	0.44 ± 0.07 $(-)$	0 $(-)$	0 $(-)$
$K^{*-} \pi^+$	15.21 ± 3.83 $(-)$	-0.038 ± 0.041 $(-)$	$-$
$\bar{K}^{*0} \pi^0$	4.27 ± 1.36 $(-)$	-0.064 ± 0.146 $(-)$	$-$
$\bar{K}^{*0} \eta$	3.26 ± 0.93 $(-)$	0.730 ± 0.108 $(-)$	$-$
$\bar{K}^{*0} \eta'$	1.99 ± 0.47 $(-)$	-0.794 ± 0.191 $(-)$	$-$
$K^{*-} K^+$	7.79 ± 0.86 $(-)$	0.073 ± 0.079 $(-)$	$-$
$K^{*+} K^-$	8.79 ± 0.66 $(-)$	-0.018 ± 0.054 $(-)$	$-$
$\bar{K}^{*0} K^0$	5.74 ± 0.63 $(-)$	0 $(-)$	$-$
$K^{*0} \bar{K}^0$	9.54 ± 0.66 $(-)$	0 $(-)$	$-$

Table 6. Predicted B_s decay observables in Scheme (B2). Numbers in the parentheses are the pulls of theory predictions from the current experimental data.

Based on our best fits, we calculate all observables in the $B \to VP$ decays. The part for B_s decays is particularly useful because currently no such observables have been observed yet and our results serve as predictions to be compared with.

Acknowledgments

References

[1] N. Cabibbo, *Unitary symmetry and leptonic decays*, *Phys. Rev. Lett.* **10** (1963) 531 [SPIRES].

[2] M. Kobayashi and T. Maskawa, *CP violation in the renormalizable theory of weak interaction*, *Prog. Theor. Phys.* **49** (1973) 652 [SPIRES].

[3] D. Zeppenfeld, SU(3) *relations for B meson decays*, *Z. Phys.* **C 8** (1981) 77 [SPIRES].

[4] M.J. Savage and M.B. Wise, SU(3) *predictions for nonleptonic B meson decays*, *Phys. Rev.* **D 39** (1989) 3346 [*Erratum ibid.* **D 40** (1989) 3127] [SPIRES].

[5] L.L. Chau, H.Y. Cheng, W.K. Sze, H. Yao and B. Tseng, *Charmless nonleptonic rare decays of B mesons*, *Phys. Rev.* **D 43** (1991) 2176 [*Erratum ibid.* **D 58** (1998) 019902] [SPIRES].

[6] M. Gronau, O.F. Hernandez, D. London and J.L. Rosner, *Decays of B mesons to two light pseudoscalars*, *Phys. Rev.* **D 50** (1994) 4529 [hep-ph/9404283] [SPIRES].

[7] M. Gronau, O.F. Hernandez, D. London and J.L. Rosner, *Electroweak penguins and two-body B decays*, *Phys. Rev.* **D 52** (1995) 6374 [hep-ph/9504327] [SPIRES].

[8] C.-W. Chiang and Y.-F. Zhou, *Flavor* SU(3) *analysis of charmless B meson decays to two pseudoscalar mesons*, *JHEP* **12** (2006) 027 [hep-ph/0609128] [SPIRES].

[9] G. Kramer, W.F. Palmer and H. Simma, *CP violation and strong phases from penguins in $B^\pm \to PP$ and $B^\pm \to VP$ decays*, *Z. Phys.* **C 66** (1995) 429 [hep-ph/9410406] [SPIRES].

[10] N.G. Deshpande, B. Dutta and S. Oh, *Branching ratios and CP asymmetries of B decays to a vector and a pseudoscalar meson*, *Phys. Lett.* **B 473** (2000) 141 [hep-ph/9712445] [SPIRES].

[11] A. Ali, G. Kramer and C.-D. Lu, *Experimental tests of factorization in charmless non-leptonic two-body B decays*, *Phys. Rev.* **D 58** (1998) 094009 [hep-ph/9804363] [SPIRES].

[12] M.-Z. Yang and Y.-D. Yang, $B \to PV$ *decays in QCD improved factorization approach*, *Phys. Rev.* **D 62** (2000) 114019 [hep-ph/0007038] [SPIRES].

[13] D.-s. Du, H.-j. Gong, J.-f. Sun, D.-s. Yang and G.-h. Zhu, *Phenomenological analysis of charmless decays $B \to PV$ with QCD factorization*, *Phys. Rev.* **D 65** (2002) 094025 [hep-ph/0201253] [*Erratum ibid.* **D 66** (2002) 079904] [SPIRES].

[14] J.-f. Sun, G.-h. Zhu and D.-s. Du, *Phenomenological analysis of charmless decays $B_s \to PP, PV$ with QCD factorization*, *Phys. Rev.* **D 68** (2003) 054003 [hep-ph/0211154] [SPIRES].

[15] R. Aleksan, P.F. Giraud, V. Morenas, O. Pene and A.S. Safir, *Testing QCD factorisation and charming penguins in charmless $B \to PV$*, *Phys. Rev.* **D 67** (2003) 094019 [hep-ph/0301165] [SPIRES].

[16] M. Beneke and M. Neubert, *QCD factorization for $B \to PP$ and $B \to PV$ decays*, *Nucl. Phys.* **B 675** (2003) 333 [hep-ph/0308039] [SPIRES].

[17] X.-q. Li and Y.-d. Yang, *Reexamining charmless $B \to PV$ decays in QCD factorization approach*, *Phys. Rev.* **D 73** (2006) 114027 [hep-ph/0602224] [SPIRES].

[18] C.-D. Lu and M.-Z. Yang, $B \to \pi\rho, \pi\omega$ *decays in perturbative QCD approach*, *Eur. Phys. J.* **C 23** (2002) 275 [hep-ph/0011238] [SPIRES].

[19] C.-H. Chen, Y.-Y. Keum and H.-n. Li, *Perturbative QCD analysis of $B \to \phi K$ decays*, *Phys. Rev.* **D 64** (2001) 112002 [hep-ph/0107165] [SPIRES].

[20] X. Liu, H.-s. Wang, Z.-j. Xiao, L. Guo and C.-D. Lu, *Branching ratio and CP asymmetry of $B \to \rho\eta^{(')}$ decays in the perturbative QCD approach*, *Phys. Rev.* **D 73** (2006) 074002

[hep-ph/0509362] [SPIRES].

[21] L. Guo, Q.-g. Xu and Z.-j. Xiao, *B → KK* decays in the perturbative QCD approach*, *Phys. Rev.* **D 75** (2007) 014019 [hep-ph/0609005] [SPIRES].

[22] D.-Q. Guo, X.-F. Chen and Z.-J. Xiao, *B⁰ → ωη⁽ʹ⁾ and φη⁽ʹ⁾ decays in the perturbative QCD approach*, *Phys. Rev.* **D 75** (2007) 054033 [hep-ph/0702110] [SPIRES].

[23] A. Ali et al., *Charmless non-leptonic B_s decays to PP, PV and VV final states in the pQCD approach*, *Phys. Rev.* **D 76** (2007) 074018 [hep-ph/0703162] [SPIRES].

[24] W. Wang, Y.-M. Wang, D.-S. Yang and C.-D. Lu, *Charmless two-body $B(B_s) → VP$ decays in soft-collinear-effective-theory*, *Phys. Rev.* **D 78** (2008) 034011 [arXiv:0801.3123] [SPIRES].

[25] A.S. Dighe, M. Gronau and J.L. Rosner, *B decays to charmless VP final states*, *Phys. Rev.* **D 57** (1998) 1783 [hep-ph/9709223] [SPIRES].

[26] M. Gronau and J.L. Rosner, *New information on B decays to charmless VP final states*, *Phys. Rev.* **D 61** (2000) 073008 [hep-ph/9909478] [SPIRES].

[27] M. Gronau, *Electroweak penguin amplitudes and constraints on gamma in charmless $B → VP$ decays*, *Phys. Rev.* **D 62** (2000) 014031 [SPIRES].

[28] C.-W. Chiang, M. Gronau, Z. Luo, J.L. Rosner and D.A. Suprun, *Charmless $B → VP$ decays using flavor* SU(3) *symmetry*, *Phys. Rev.* **D 69** (2004) 034001 [hep-ph/0307395] [SPIRES].

[29] Updated results and references are tabulated periodically by the Heavy Flavor Averaging Group: http://www.slac.stanford.edu/xorg/hfag/rare.

[30] BABAR collaboration, B. Aubert et al., *Measurements of branching fractions and CP-violating asymmetries in $B^0 → ρ^± h^∓$ decays*, *Phys. Rev. Lett.* **91** (2003) 201802 [hep-ex/0306030] [SPIRES]; *Measurements of branching fractions in $B → φK$ and $B → φπ$ and search for direct CP-violation in $B^± → φK^±$*, *Phys. Rev.* **D 69** (2004) 011102 [hep-ex/0309025] [SPIRES]; *Measurement of branching fractions and charge asymmetries in $B^± → ρ^± π^0$ and $B^± → ρ^0 π^±$ decays and search for $B^0 → ρ^0 π^0$*, *Phys. Rev. Lett.* **93** (2004) 051802 [hep-ex/0311049] [SPIRES]; *Evidence for the decay $B^± → K^{*±} π^0$*, *Phys. Rev.* **D 71** (2005) 111101 [hep-ex/0504009] [SPIRES]; *An amplitude analysis of the decay $B^± → π^± π^± π^∓$*, *Phys. Rev.* **D 72** (2005) 052002 [hep-ex/0507025] [SPIRES]; *Dalitz plot analysis of the decay $B^± → K^± K^± K^∓$*, *Phys. Rev.* **D 74** (2006) 032003 [hep-ex/0605003] [SPIRES]; *Search for $B^+ → φπ^+$ and $B^0 → φπ^0$ decays*, *Phys. Rev.* **D 74** (2006) 011102 [hep-ex/0605037] [SPIRES]; *Search for the decay of a B^0 or $\bar{B}^0$ meson to $K^{*0} K^0$ or $K^{*0} \bar{K}^0$*, *Phys. Rev.* **D 74** (2006) 072008 [hep-ex/0606050] [SPIRES]; *Observation of $B → η' K^*$ and evidence for $B^+ → η' ρ^+$*, *Phys. Rev. Lett.* **98** (2007) 051802 [hep-ex/0607109] [SPIRES]; *Measurement of branching fractions and charge asymmetries in B decays to an eta meson and a K^* meson*, *Phys. Rev. Lett.* **97** (2006) 201802 [hep-ex/0608005] [SPIRES]; *Measurement of the CP asymmetry and branching fraction of $B^0 → ρ^0 K^0$*, *Phys. Rev. Lett.* **98** (2007) 051803 [hep-ex/0608051] [SPIRES]; *Measurement of the $B^± → ρ^± π^0$ branching fraction and direct CP asymmetry*, *Phys. Rev.* **D 75** (2007) 091103 [hep-ex/0701035] [SPIRES]; *Observation of $B^+ → ρ^+ K^0$ and measurement of its branching fraction and charge asymmetry*, *Phys. Rev.* **D 76** (2007) 011103 [hep-ex/0702043] [SPIRES]; *Search for neutral B-meson decays to $a_0 π$, $a_0 K$, $ηρ^0$ and $ηf_0$*, *Phys. Rev.* **D 75** (2007) 111102 [hep-ex/0703038] [SPIRES]; *Search for the decay $B^+ → \bar{K}^{*0}(892)K^+$*, *Phys. Rev.* **D 76** (2007) 071103

[arXiv:0706.1059] [SPIRES]; *Branching fraction and CP-violation charge asymmetry measurements for B-meson decays to $\eta K^p m$, $\eta \pi^\pm$, $\eta' K$, $\eta' \pi^\pm$, ωK and $\omega \pi^\pm$*, *Phys. Rev.* **D 76** (2007) 031103 [arXiv:0706.3893] [SPIRES]; *Dalitz plot analysis of the decay $B^0(\bar{B}^0) \to K^\pm \pi^\mp \pi^0$*, *Phys. Rev.* **D 78** (2008) 052005 [arXiv:0711.4417] [SPIRES]; *Evidence for direct CP-violation from Dalitz-plot analysis of $B^\pm \to -> K^\pm \pi^\mp \pi^\pm$*, *Phys. Rev.* **D 78** (2008) 012004 [arXiv:0803.4451] [SPIRES]; *Observation of $B^+ \to \eta \rho^+$ and search for B^0 decays to $\eta' \eta$, $\eta \pi^0$, $\eta' \pi^0$ and $\omega \pi^0$*, *Phys. Rev.* **D 78** (2008) 011107 [arXiv:0804.2422] [SPIRES]; *Amplitude analysis of the decay $B^0 \to K^+ \pi^- \pi^0$*, arXiv:0807.4567 [SPIRES].

[31] BELLE collaboration, A. Gordon et al., *Study of $B \to \rho \pi$ decays at Belle*, *Phys. Lett.* **B 542** (2002) 183 [hep-ex/0207007] [SPIRES]; BELLE collaboration, K.F. Chen et al., *Measurement of branching fractions and polarization in $B \to \phi K^{(*)}$ decays*, *Phys. Rev. Lett.* **91** (2003) 201801 [hep-ex/0307014] [SPIRES]; BELLE collaboration, J. Zhang et al., *Measurement of branching fraction and CP asymmetry in $B^+ \to \rho^+ \pi^0$*, *Phys. Rev. Lett.* **94** (2005) 031801 [hep-ex/0406006] [SPIRES]; BELLE collaboration, P. Chang et al., *Observation of the decays $B^0 \to K^+ \pi^- \pi^0$ and $B^0 \to \rho^- K^+$*, *Phys. Lett.* **B 599** (2004) 148 [hep-ex/0406075] [SPIRES]; BELLE collaboration, A. Garmash et al., *Dalitz analysis of the three-body charmless decays $B^+ \to K^+ \pi^+ \pi^-$ and $B^+ \to K^+ K^+ K^-$*, *Phys. Rev.* **D 71** (2005) 092003 [hep-ex/0412066] [SPIRES]; *Dalitz analysis of three-body charmless $B^0 \to K^0 \pi^+ \pi^-$ decay*, *Phys. Rev.* **D 75** (2007) 012006 [hep-ex/0610081] [SPIRES]; BELLE-COLLABORATION collaboration, K. Abe et al., *Measurements of branching fractions and polarization in $B \to K^* \rho$ decays*, *Phys. Rev. Lett.* **95** (2005) 141801 [hep-ex/0408102] [SPIRES]; A. Garmash et al., *Evidence for large direct CP-violation in $B^\pm \to \rho(770)^0 K^\pm$ from analysis of the three-body charmless $B^\pm \to K^\pm \pi^\pm \pi^\pm$ decay*, *Phys. Rev. Lett.* **96** (2006) 251803 [hep-ex/0512066] [SPIRES]; BELLE collaboration, C.M. Jen et al., *Improved measurements of branching fractions and CP partial rate asymmetries for $B \to \omega K$ and $B \to \omega \pi$*, *Phys. Rev.* **D 74** (2006) 111101 [hep-ex/0609022] [SPIRES]; BELLE collaboration, C.H. Wang et al., *Measurement of charmless B decays to ηK^* and $\eta \rho$*, *Phys. Rev.* **D 75** (2007) 092005 [hep-ex/0701057] [SPIRES]; J. Schumann et al., *Search for B decays into $\eta' \rho$, $\eta' K^*$, $\eta' \phi$, $\eta' \omega$ and $\eta' \eta^{(\prime)}$*, *Phys. Rev.* **D 75** (2007) 092002 [hep-ex/0701046] [SPIRES]; BELLE collaboration, A. Kusaka et al., *Measurement of CP asymmetries and branching fractions in a time-dependent Dalitz analysis of $B^0 \to (\rho \pi)^0$ and a constraint on the quark mixing angle ϕ_2*, *Phys. Rev.* **D 77** (2008) 072001 [arXiv:0710.4974] [SPIRES]; BELLE collaboration, I. Adachi et al., *Studies of Direct CP violation in three-body charmless $B^\pm \to K^\pm \pi^\pm \pi^\mp$ decays*, Belle BELLE-CONF-0827 (2008).

[32] CDF collaboration, D.E. Acosta et al., *First evidence for $B_s^0 \to \phi \phi$ decay and measurements of branching ratio and A_{CP} for $B^+ \to \phi K^+$*, *Phys. Rev. Lett.* **95** (2005) 031801 [hep-ex/0502044] [SPIRES].

[33] CLEO collaboration, D.M. Asner et al., *Search for exclusive charmless hadronic B decays*, *Phys. Rev.* **D 53** (1996) 1039 [hep-ex/9508004] [SPIRES]; CLEO collaboration, R.A. Briere et al., *Observation of $B \to \phi K$ and $B \to \phi K^*$*, *Phys. Rev. Lett.* **86** (2001) 3718 [hep-ex/0101032] [SPIRES]; CLEO collaboration, T. Bergfeld et al., *Observation of $B^+ \to \omega K^+$ and search for related B*

decay modes, *Phys. Rev. Lett.* **81** (1998) 272 [`hep-ex/9803018`] [SPIRES];
CLEO collaboration, S.J. Richichi et al., *Two-body B meson decays to η and $\eta^{'}$: observation of $B \to \eta K^*$*, *Phys. Rev. Lett.* **85** (2000) 520 [`hep-ex/9912059`] [SPIRES];
CLEO collaboration, S. Chen et al., *Measurement of charge asymmetries in charmless hadronic B meson decays*, *Phys. Rev. Lett.* **85** (2000) 525 [`hep-ex/0001009`] [SPIRES];
CLEO collaboration, C.P. Jessop et al., *Study of charmless hadronic B meson decays to pseudoscalar vector final states*, *Phys. Rev. Lett.* **85** (2000) 2881 [`hep-ex/0006008`] [SPIRES];
CLEO collaboration, E. Eckhart et al., *Observation of $B \to K_S^0 pi^+ pi^-$ and evidence for $B \to K^{*\pm} \pi^{\mp}$*, *Phys. Rev. Lett.* **89** (2002) 251801 [`hep-ex/0206024`] [SPIRES];
CLEO collaboration, B.I. Eisenstein et al., *Measurement of the charge asymmetry in $B \to K^*(892)^{\pm}\pi^{\mp}$*, *Phys. Rev.* **D 68** (2003) 017101 [SPIRES].

[34] PARTICLE DATA GROUP collaboration, S. Eidelman et al., *Review of particle physics*, *Phys. Lett.* **B 592** (2004) 1 [SPIRES] and 2005 partial update for the 2006 edition available on the PDG WWW pages http://pdg.lbl.gov/.

[35] L. Wolfenstein, *Parametrization of the Kobayashi-Maskawa Matrix*, *Phys. Rev. Lett.* **51** (1983) 1945 [SPIRES].

[36] CKMFITTER GROUP collaboration, J. Charles et al., *CP violation and the CKM matrix: assessing the impact of the asymmetric B factories*, *Eur. Phys. J.* **C 41** (2005) 1 [`hep-ph/0406184`] [SPIRES]; updated results may be found on the web site: http://ckmfitter.in2p3.fr/.

[37] C.-W. Chiang, M. Gronau, J.L. Rosner and D.A. Suprun, *Charmless $B \to PP$ decays using flavor* SU(3) *symmetry*, *Phys. Rev.* **D 70** (2004) 034020 [`hep-ph/0404073`] [SPIRES].

[38] S. Barshay, G. Kreyerhoff and L.M. Sehgal, *Direct CP-violation in $B^{\mp} \to \pi^{\mp}\omega$, $\pi^{\mp}\rho^0$, $\pi^0\rho^{\mp}$ and in $\bar{B}^0(B^0) \to \pi^{\mp}\rho^{\pm}$ with an enhanced branching ratio for $\pi^0\rho^0$*, *Phys. Lett.* **B 595** (2004) 318 [`hep-ph/0405012`] [SPIRES].

[39] Y.-L. Wu and Y.-F. Zhou, *Implications of charmless B decays with large direct CP-violation*, *Phys. Rev.* **D 71** (2005) 021701 [`hep-ph/0409221`] [SPIRES].

[40] Y.-Y. Charng and H.-n. Li, *Weak phases from the $B \to \pi\pi$, $K\pi$ decays*, *Phys. Rev.* **D 71** (2005) 014036 [`hep-ph/0410005`] [SPIRES].

[41] X.-G. He and B.H.J. McKellar, *Hadron decay amplitudes from $B \to K\pi$ and $B \to \pi\pi$ decays*, `hep-ph/0410098` [SPIRES].

[42] Y.-L. Wu and Y.-F. Zhou, *Charmless decays $B \to \pi\pi$, πK and KK in broken* SU(3) *symmetry*, *Phys. Rev.* **D 72** (2005) 034037 [`hep-ph/0503077`] [SPIRES].

[43] Y.-L. Wu, Y.-F. Zhou and C. Zhuang, *Constraining charming penguins in charmless B decays*, `arXiv:0712.2889` [SPIRES].

[44] H.J. Lipkin, *Penguins, trees and final state interactions in B decays in broken* SU(3), *Phys. Lett.* **B 415** (1997) 186 [`hep-ph/9710342`] [SPIRES].

[45] H.J. Lipkin, *FSI rescattering in $B^{\pm}$ decays via states with η, $\eta^{'}\omega$ and ϕ*, *Phys. Lett.* **B 433** (1998) 117 [SPIRES].

[46] H.J. Lipkin, *New systematics in charmless strange $B^+ \to VP$ decays*, `arXiv:0705.2557` [SPIRES].

[47] UTFIT collaboration, M. Bona et al., *The 2004 UTfit Collaboration report on the status of*

the unitarity triangle in the standard model, *JHEP* **07** (2005) 028 [`hep-ph/0501199`] [SPIRES]; updated results may be found on the web site: http://utfit.roma1.infn.it/.

[48] N.G. Deshpande, X.-G. He and J.-Q. Shi, SU(3) *flavor symmetry and CP-violating rate differences for charmless $B \to PV$ decays*, *Phys. Rev.* **D 62** (2000) 034018 [`hep-ph/0002260`] [SPIRES].

[49] M. Iwasaki, *Measurements of charmless B decays at Belle*, talk presented at the *ICHEP 2008 Conference*, Philadelphia PA July 29 – August 5 2008.